METEOR TRAIL DRIFT RESEARCH BASED ON BASELINE OBSERVATIONS

K.I. Ivanov
Irkutsk State University,
Irkutsk, Russia, ivorypalace@gmail.com

E.S. Komarova
Irkutsk State University,
Irkutsk, Russia, eskomarik@gmail.com

R.V. Vasilyev
Institute of Solar-Terrestrial Physics SB RAS,
Irkutsk, Russia, roman_vasilyev@iszf.irk.ru

M.V. Eselevich
Institute of Solar-Terrestrial Physics SB RAS,
Irkutsk, Russia, mesel@iszf.irk.ru

A.V. Mikhalev
Institute of Solar-Terrestrial Physics SB RAS,
Irkutsk, Russia, mikhalev@iszf.irk.ru

Abstract. We analyze the results of a rare long-lived quasisymmetric ellipsoidal-annular meteor trail recorded on November 18, 2017 by two optical all-sky cameras, spaced at a distance of 150 km. The analysis is based on astrometric processing results with the use of baseline measurement methods. We determine spatial-kinematic characteristics of the meteor trail, and find features of its evolution. The ignition and extinction heights of the meteor were in the range 75–120 km. The estimate of the meteor brightness gives the absolute magnitude of about –7.3 $^{\text{m}}$. It is shown that the distribution of all parts of the long-lived meteor trail occurs in the same plane at a height of ~90 km at a speed of ~320 m/s and, apparently, cannot be a consequence of an air mass movement. The total time of the meteor trail observation was more than 30 min. We offer possible explanations for the results obtained in the context of upper atmosphere processes.

Keywords: meteor, long-lived meteor trail, baseline observations, astrometry, upper atmosphere, shock wave.

INTRODUCTION

The topicality of the meteor astronomy has increased markedly over the past decade. This is partly due to the appearance of new methods for recording and processing images, which can examine phenomena accompanying a meteoroid passage through the upper atmosphere. These methods allow us to study physical-chemical characteristics both of meteor particles and of the surrounding matter. Among still open questions is the determination of physical parameters and masses of meteoroids, their spatial distribution, chemical composition, origin, structure and evolution of meteor showers and the Solar System as a whole, asteroid and comet impact hazards, and the possibility of using meteors for atmospheric sounding.

Of particular importance in the context of the latter problem are the so-called bolides – bright meteors that have, as a rule, an extended trajectory and appear when large meteoroids enter Earth's atmosphere: the set of characteristics of phenomena of this type is most favorable for recording and follow-up study, which ultimately gives high-quality results being of keen scientific interest. Furthermore, long-lived ionization trails, which often accompany bolides, can provide valuable information on processes occurring in the upper atmosphere [Kelley et al., 2000].

This paper examines a bolide recorded on November 18, 2017 and accompanied by the formation of a long-lived ionization meteor trail of rare quasisymmetric ellipsoidal-annular form. We perform an astrometric analysis of the meteor and its trail, using baseline observations. We discuss possible mechanisms of the formation and propagation of the trail.

MAIN CHARACTERISTICS OF OBSERVING STATIONS

A bright meteor was observed over the territory of Eastern Sayan and Tunka Valley on November 18, 2017. The event was recorded by two all-sky cameras spaced a distance of 150 km at Sayan Solar Observatory (SSO) and Geophysical Observatory (GPhO) of the Institute of Solar-Terrestrial Physics SB RAS. The main information on the observing stations and equipment is given in Table 1.

Table 1

Some characteristics of observing stations

	Station 1	Station 2
Name	SSO	GPhO
Coordinates	51°37′18″ N, 100°55′07″ E	51°48′39″ N, 103°04′56″ E
Camera	SBIG AllSky-340	KEO Sentinel
Exposition	60 s	60 s
Pixel resolution	640×480	511×511
Image scale	18′/pixel	21′/pixel

Simultaneous observations from two stations spaced at a sufficiently large distance, the so-called baseline observations, allow us to estimate many physical parameters of the meteor. Such studies generally place rather high demands on the equipment, in particular on resolution and frame rate. In our case, both the parameters have a small value; however, we managed to obtain high-quality images of the meteor trail and identify a number of its characteristics.

MAIN PARAMETERS OF THE METEOR UNDER STUDY

The event occurred on November 18, 2017 between 22:23:19 and 22:24:20 UT. Due to the long exposure time of both the cameras and the absence of other information, it is impossible to determine the time of the passage of the meteor more accurately. Images of the meteor are presented in Figure 1. Both the images show a bright trail whose brightness increases uniformly along the path of the meteoroid and ends abruptly. This corresponds to ablation of the meteoroid in rarefied atmospheric layers with a subsequent flash.

Due to the considerable exposure time, we cannot directly measure the speed of the meteoroid; however, the orientation of the trail when detected allows us to conclude that it belongs to the well-studied Leonids meteor shower, whose average velocity of particles in Earth's atmosphere is known to be ~70 km/s [Babadjanov, 1987].

Lack of data on the exposure time of the trail also makes it impossible to accurately determine the meteor brightness. Nevertheless, the approximate analysis carried out using the software package IRAF [Tody, 1993] yields the absolute magnitude of about -7.3^m; hence, the meteor of interest is a bolide. Astrometric measurements made using the software package Astrometry.net [Lang et al., 2010] give estimated values of the begin and end coordinates of the meteor trail, converted into the azimuth frame of reference for the convenience of further calculations. Table 2 lists the main astrometric parameters of the meteor trail, determined from the 3σ criterion above the background: azimuth along the meteor trail (A_m); azimuths to the begin (A_{begin}) and end (A_{end}) points of the trail; heights of the begin (h_{begin}) and end (h_{end}) points of the trail above the horizon; angular length of the trail (l).
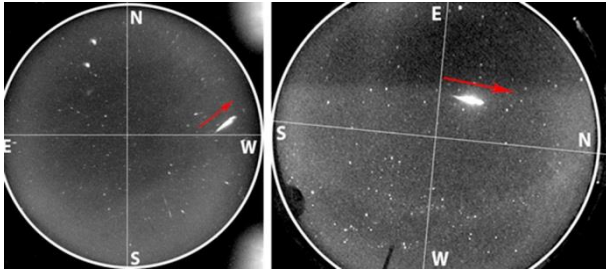

Figure 1. Meteor images obtained on November 18, 2017 at 22:24:20 UT with cameras installed at GPhO (left) and SSO (right). The meteor path is indicated by an arrow

Table 2

Main astrometric parameters of the meteor under study

Parameter	SSO	GPhO
A_m, deg.	353.4±2.8	311.3±3.2
A_{begin}, deg.	69.6±3.1	272.6±2.2
A_{end}, deg.	40.7±2.9	280.0±3.0
h_{begin}, deg.	60.2±2.5	23.5±3.9
h_{end}, deg.	50.6±2.9	12.3±4.6
l, deg.	18.9±3.2	15.3±4.5
visible brightness	-7.4^m±1.5	-6.6^m±1.9

DETERMINING THE MAIN GEOMETRIC CHARACTERISTICS OF THE METEOR TRAIL

The results presented in the previous section make it possible to determine the height of the begin and end points of the meteor trail, the distance to each of them along the line of sight, as well as its visible length. To calculate these parameters, it is convenient to use a horizontal coordinate system connected with Earth's surface and the method described in [Katasev, 1957]. According to this source, we can find the height H of any point of the meteor trail from baseline observations, using the formula

$$
\begin{cases}
H = b \dfrac{\sin \alpha_2}{\sin \gamma} ctg\, Z_A = b \dfrac{\sin \alpha_1}{\sin \gamma} ctg\, Z_B; \\
\alpha_1 = \alpha_0 - \alpha_A; \\
\alpha_2 = \alpha_B - \alpha_0; \\
\gamma = 180° - (\alpha_1 + \alpha_2),
\end{cases}
\tag{1}
$$

where b is the baseline length; α_0 is the baseline azimuth; α_A and α_B are azimuths to the projection of the meteor trail point under study on Earth's surface from stations A and B; γ is the angle between these azimuths; Z_A and Z_B are zenith distances of the trail point considered.

Knowing the height H of an arbitrary point of the meteor over Earth's surface, it is easy to calculate the distance R to it along the line of sight from each observing station:

$$
R = H / \cos Z,
\tag{2}
$$

where Z is the zenith distance of the point.

Given the LOS distances to the begin and end points of the trail, determined from this formula, and its angular length l, we obtain an expression for its visible length L:

$$
L = R_{begin}^2 + R_{end}^2 - 2R_{begin}R_{end} \cos l.
\tag{3}
$$

The results of the calculations of these parameters are presented in Table 3, where H_{begin} and H_{end} are the heights of the begin and end points of the meteor path; R_{begin} and R_{end} are the distance along the line of sight from the begin and end points of the meteor trail respectively; L is the visible length of the trail.

Table 3

Heights and distances along the line of sight for the begin and end points of the meteor path, determined from the criterion 3σ above the background level

Parameter	SSO	GPhO	Average
H_{begin}, km	108.8±8.3	118.4±7.8	113.6±8.0
H_{end}, km	76.4±8.5	77.3±9.8	76.9±9.2
R_{begin}, km	125.6±9.1	–	–
R_{end}, km	98.9±8.8	–	–
L, km	45.3±7.4	–	–

As seen from Table 3, mean values of the ignition and extinction heights of the meteor are within 75–120 km, which is typical of the vast majority of meteoroids.

Due to the proximity of the trail to the horizon, low resolution of the image, and considerable distortion of the image at the edge of the frame, L, R_{begin}, and R_{end} for GPhO are determined with an error of more than ±50 km and therefore are not shown.

STUDYING THE LONG-LIVED METEOR TRAIL DRIFT

The considerable brightness is not the only feature of the meteor under study. It also left a bright quasisymmetric trail presumably of ionization nature, observed during at least 30 min after the moment of detection of the event. Despite the low brightness compared to nearby stars, the trail was clearly seen in red and drifted against the stars, gradually transforming under the influence of external conditions. The analysis of the trail drift performed below leads to some interesting conclusions about the nature of the processes occurring in the upper atmosphere [Astapovich, 1958; Bronstein, 1981; Kashcheev et al., 1967].

Figure 2 presents the meteor trail images obtained at both the observatories 5 min after the detection of the event. We can clearly see the trail in the form of a loop. The visual analysis of the images does not allow us to draw conclusions about the nature of the processes that caused the deformation, but the available data are sufficient for the mathematical analysis.

Unfortunately, because of the proximity to the horizon we cannot examine the image captured at the territory of the GPhO site – we can only employ it as a reference in determining heights, the further analysis will be conducted using SSO images.

For convenience in the analysis, the meteor trail is shown in white. We can clearly see a relatively even quasisymmetric propagation of the trail in all directions, an increase in its length and cross-section. The last result is likely to be due exclusively to diffusion of the meteoric material in the ambient gas, while the first two could be due to its transfer both by currents of the atmosphere and directly by the shock wave, generated by the bolide when it flashed.

Despite the apparent uniform expansion of the trail remains, of greatest interest are points 1 and 3 (presumably the begin and end points of the path respectively), as well as point of inflexion 2, the formation of which may be associated with a change in the direction of air mass movement. The direction of the drift of each point is indicated by an arrow, stages of the evolution of the trail from earlier to later are designated by the letters a–d.

Using the method described in Section 3, we succeeded in determining heights for the three directions of trail propagation with an estimated accuracy of 5 km.
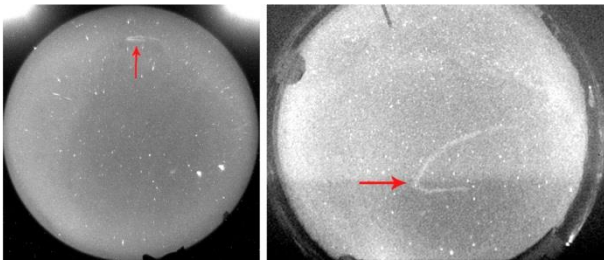

Figure 2. Deformation of the meteor trail 5 min after the event as derived from images obtained at GPhO (left) and SSO (right)

Figure 3 shows a composite image obtained by summing the first five frames containing meteor and trail images. The calculation results are presented in Table 4.

As is seen from Table 4, the calculated heights for all the trail drift stages considered for one direction are within the measurement accuracy. This allows us to confirm the horizontal transfer and the absence of the marked vertical air mass movement. The characteristic size of the expanding trail region was as large as ~400 km. To describe the process in detail requires data on the velocity of propagation of a disturbance relative to Earth's surface. Expressing the distance from the observation point to the projection of an arbitrary point of the meteor trail on Earth's surface in terms of the height and zenith angle values calculated at the previous stages, we have:

$$r = H \mathrm{tg} Z. \qquad (4)$$

To determine the full velocity vector, it is convenient to use a rectangular coordinate system related to Earth's surface. Then the position of the projection of the arbitrary point of the trail on Earth's surface is uniquely determined by two coordinates:

$$\begin{cases} x = r\sin\alpha = H\mathrm{tg}Z\sin\alpha, \\ y = r\cos\alpha = h\mathrm{tg}Z\cos\alpha, \end{cases} \qquad (5)$$

where α is the azimuth from the observing station to the point of meteor trail projection; Z is the zenith distance of its associated point of the trail.

In view of formula (5), the full velocity vector is found as follows

$$\upsilon = \sqrt{\left(\frac{\Delta x}{\Delta t}\right)^2 + \left(\frac{\Delta y}{\Delta t}\right)^2}. \qquad (6)$$

The calculation results are presented in Table 5.

Attention is drawn to high velocities of disturbance propagation: in direction 3 they were on average by 20 % and in directions 1 and 2 by 30% higher than the calculated velocity of sound at the given height according to the standard atmosphere model. Similar results with a high degree of probability suggest that the observed glow is localized at the shock wave front and propagates with it in the thin atmospheric layer located at a height of ~90 km.
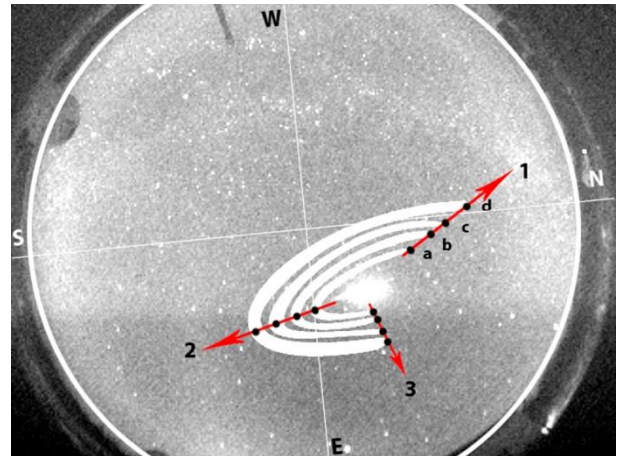

Figure 3. Modification and drift of the meteor trail under atmospheric conditions

Table 4

Calculated heights for three key points of the meteor trail.

Height, km	Direction 1	Direction 2	Direction 3
Trail a	95.8±5.1	93.2±5.8	89.4±4.8
Trail b	94.0±4.9	90.9±6.1	85.1±5.5
Trail c	91.7±5.6	90.1±5.6	93.3±5.3
Trail d	90.8± 5.8	92.6±6.2	91.0±5.0
Average	92.9±5.4	91.7±59	89.7±5.2

Table 5

Values of the total velocity vector for the trail path sections under studied.

Speed m/s	Direction 1	Direction 2	Direction 3
a–b	322.5±27.2	324.6±23.9	311.9±20.7
b–c	316.8±27.1	317.9±25.7	298.7±21.0
c–d	330.3±28.4	327.5±24.8	308.4±21.8
aver	323.2±27.6	323.3±24.8	306.0±21.2

As for the spectrum of the meteor trail brightness we can say that it may be due both to the glow of the meteoric material and to atmospheric components. In terms of the yellowish tinge of the meteor trail on the images obtained by a color camera, it seems interesting to note the possible contribution of both the atmospheric sodium layer, localized at comparable heights, and meteoric material, which may also contain Na, to the integral brightness of the trail. The last assumption is supported by images obtained in different spectral channels (Figure 4).

The maximum intensity of the meteor trail light emission is detected in red, while in blue its value is almost at the background level. In this case, the trail of the bolide is well defined in all channels.
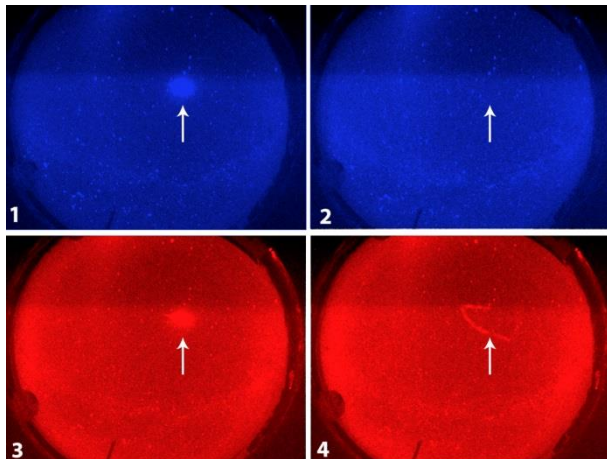

Figure 4. Images of the meteor trail and initial stage of trail propagation in blue (frames 1 and 2) and red (frames 3 and 4) channels, taken practically simultaneously. In blue (frame 2), the trail is hardly seen

CONCLUSIONS

We have studied a bright bolide leaving a trail detected within half an hour after the event and propagating symmetrically in all directions with a supersonic velocity of about 320 m/s. The initial assumption about the possible formation of the phenomenon due to the interaction between the ionization meteor trail and air flows is inconsistent with the calculation results and apparently is untenable. This can be confirmed by neutral wind measurements made at GPhO during this period with the Fabry-Perot interferometer in the 557.7 nm atomic oxygen [OI] line (85–115 km meteor glow height) [Vasilyev et al., 2017].

During the formation and development of the long-lived meteor trail, the northward wind with characteristic velocities of 60–80 m/s prevailed, and it seems to be impossible to explain quasisymmetric propagation of the trail by its influence.

A much more plausible assumption is that the disturbance had the wave nature. In this case, the observed glow can be localized directly in the shock front, generated by the meteor flash and propagating with a velocity of ~320 m/s in a thin atmospheric layer at a height of ~90 km. For example, it is known that a weak shock wave moves through the undisturbed gas at a velocity very close to the velocity of sound, i.e. it is virtually identical to the acoustic compression wave [Landau and Lifshitz, 1986; Zeldovich, Reiser, 2008]. In the far-field zone from the site of generation of the shock wave providing that it propagates horizontally, when parameters of the undisturbed medium remain virtually unchanged, its velocity under certain conditions (e.g., under slight dissipation for a weak shock wave) may vary a little, asymptotically approaching the velocity of sound [Pinaev et al., 2000]. An indirect confirmation of this mechanism can be considered the coincidence of calculated heights of the flash and drifting trail.

We also do not rule out the mechanism of the formation of the meteoroid explosion at the initial stage under the action of a shock wave or explosion itself relative to the thin spherical layer of meteoric material, which received a sufficiently large initial impulse. The estimates show that due to the impulse meteor particles can propagate in a horizontal direction in a particular range of heights without velocity attenuation over distances as long as tens or hundreds of kilometers [Platov et al., 2013]. In this case, the above feature of the observed wind (assuming that it remained unchanged at the meteor glow height) might have formed a trail image as a semi-ellipse. The brightest part of the meteor trail corresponds to the southward movement, against the incoming wind stream.

REFERENCES

Astapovich I.S. *Meteornye yavleniya v atmosfere Zemli* [Meteor Phenomena in the Earth's Atmosphere]. Moscow,

State Publishing House of Physical and Mathematical Literature, 1958, 650 p. (In Russian).

Babadjanov P.B. *Meteory i ikh nablyudeniya* [Meteors and Their Observation]. Moscow, Nauka Publ., 1987, 176 p. (In Russian).

Bronstein V.A. *Fizika meteornykh yavlenii* [Physics of Meteor Phenomena]. Moscow, Nauka Publ., 1981, 416 p. (In Russian).

Kashcheev B.L., Lebedinets V.N., Lagutin M.F. *Meteornye yavleniya v atmosphere Zemli* [Meteor Phenomena in the Earth's Atmosphere]. Moscow, Nauka Publ., 1967, 260 p. (In Russian).

Katasev L.A. *Fotograficheskie metody meteornoi astronomii* [Photographic Methods of Meteoric Astronomy]. Moscow, State Publishing House of Technical and Theoretical Literature, 1957, 179 p. (In Russian).

Kelley M.C., Gardner C., Drummond J., Armstrong T., Liu A., Chu X., Papen G., Kruschwitz C., Loughmiller P., Grime B., Engelman J. First observations of long-lived meteor trains with resonance lidar and other optical instruments. *Geophys. Res. Lett*. 2000, vol. 27, iss. 13, pp. 1811–1814. DOI: 10.1029/1999GLO11175.

Landau L.D., Lifshits E.M. *Gidrodinamika. Kurs teoreticheskoi fiziki: T. 6* [Hydrodynamics. Course of Theoretical Physics: vol. VI]. Moscow. Nauka Publ., 1986, 736 p. (In Russian). English edition: Landaus L.D., Lifshitz E.M. Fluid Mechanics. Pergamon Press, 1987, 554 p. (Course of Teoretical Physics, vol. 6.).

Lang D., Hogg D., Mierle K., Blanton M., Roweis S. Astrometry.net: Blind astrometric calibration of arbitary astronomical images. *Astron. J*. 2010, vol. 139, no. 5, pp. 1782–1800. DOI: 10.1088/0004-6256/139/5/1782.

Pinaev A.V., Kuzavov V.T., Kedrinskiy V.K. The structure of shock waves in the near zone with the explosion of space charges in the air. *Applied Mechanics and Technical Physics*. 2000, vol. 41, no. 5, pp. 81–90. (In Russian).

Platov Yu.V., Chernous S.A., Alpatov V.V. Features of optical phenomena associated with launching solid-propellant ballistic missiles. *Geomagnetism and Aeronomy*. 2013, vol. 53, no. 2, pp. 209–214. (In Russian).

Tody D. IRAF in the Nineties. *Astronomical Data Analysis Software and Systems, II A.S.P. Conference Series*. 1993, vol. 52, pp. 173–183.

Vasilyev R.V., Artamonov M.F., Beletsky A.B., Zherebtsov G.A., Medvedeva I.V., Mikhalev A.V., Sirenova T.E. Registering upper atmosphere parameters in East Siberia with Fabry—Perot Interferometer KEO Scientific "Arinae". *Solar-Terr. Phys*. 2017, vol. 3, iss. 3, pp. 61–75. DOI: 10.12737/stp-33201707.

Zeldovich Ya.B., Raizer Yu.P. *Fizika udarnykh voln i vysokotemperaturnykh gidrodinamicheskikh yavlenii* [Physics of Shock Waves and High-Temperature Hydrodynamic Phenomena]. Moscow, FIZMATLIT Publ., 2008, 656 p. (In Russian).